Inertial Sensor-Based Control of Functional Electrical Stimulation in Paraplegic Cycling

Stefan Ruppin, Constantin Wiesener, Thomas Schauer

***Abstract*— A method for joint angle estimation has been developed to perform FES cycling by using a joint angle-based stimulation pattern instead of a crank angle-based method. To estimate the joint angles, the orientation estimations of four IMUs are processed. The sensors dominant rotation axes are estimated to provide the possibility of arbitrary sensor-to-segment placement of the IMUs at the lower limbs. To reduce the effect of latency between stimulation onset and muscle force reaction, a correction method has been applied. The resulting FES cycling system has been verified in simulations at different seating positions using a complex model of a FES cycling ergometer. Furthermore, experiments with a paraplegic subject were successfully carried out where no further calibration regarding the stimulation ranges had to be done. The presented system offers advantages such as an intuitive, geometry-independent stimulation pattern while enabling plug & play cycling.**

I. Introduction

Functional Electrical Stimulation (FES) in combination with closed-loop control has been successfully used in several works [1, 2, 3, 4, 5] to coordinate paralyzed muscles for FES cycling. Specific training with FES can produce significant training of the cardiovascular system and raise lower limb circulation [6] for paraplegic patients.

In most recent approaches, the crank angle is used to generate the stimulation pattern for inducing a pedaling motion. Therefore, a measurement system for the crank angle is needed, e.g. an encoder at the crank. Furthermore, the phases with positive torque regarding the crank angle have to be calibrated which depend on the seating position and the seat-to-crank distance [7, 8]. This is relevant, for instance, when the wheelchair is placed differently in front of the ergometer every day or when a new subject attends the training. A joint angle-based approach is proposed to address these drawbacks.

II. Methods

The new proposed inertial sensor-based control can be subdivided into three methods. It starts by estimating the joint angles and performing a transformation to achieve independence of geometric parametrization before specifying a stimulation pattern. Properties like arbitrary sensor-to-segment placement and plug & play abilities are claimed.

S. Ruppin, C. Wiesener (corresponding author) and T. Schauer are with the Control Systems Group, Technische Universität Berlin, Germany. (phone: +49-30-314-24094; email: wiesener@control.tu-berlin.de).

A. Joint angle estimation

In Figure 1, the fundamental geometric setting for FES cycling as well as the IMU placement are illustrated. In a first

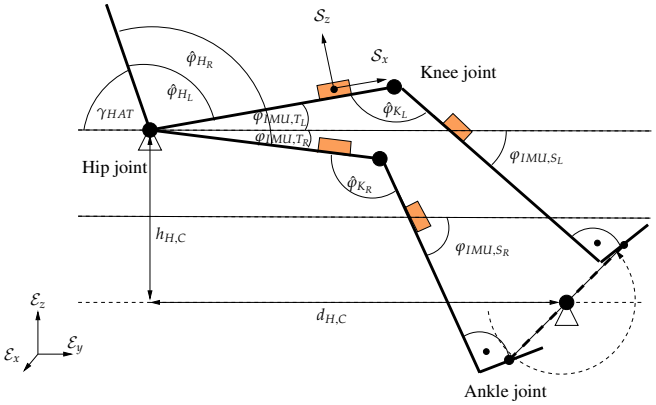

Figure 1: Geometry of the lower limbs for calculating joint angles based on inertial sensor data. Triangle formed by the thigh, shank and horizontal plane shows the estimated angles φ_{IMU,S_L}, φ_{IMU,T_L}, φ_{IMU,S_R}, φ_{IMU,T_R} and the joint angles $\hat{\varphi}_{H_R}$, $\hat{\varphi}_{K_R}$, $\hat{\varphi}_{H_L}$, $\hat{\varphi}_{K_L}$ as well as the angle of the torso γ_{HAT}.

step, the orientation quaternion ${}^{\mathcal{S}}_{\mathcal{E}}\boldsymbol{q}[k]$ at time index k is calculated for each inertial sensor using the orientation algorithm proposed in [9]. It describes the orientation of the sensor frame $\mathcal{S}$ with respect to the reference frame $\mathcal{E}$. Assuming that the ankle joints are fixed, the specific cycling motion consists mainly of an up and down motion of the sensors in the sagittal plane (more precisely: of the limb the sensor is placed on). Therefore, the azimuth free quaternion can be obtained by

$$ {}^{\mathcal{S}}_{\mathcal{A}}\boldsymbol{q}_{\mathrm{AF}}[k] = {}^{\mathcal{A}}_{\mathcal{E}}\boldsymbol{q}^{-1}_{\mathrm{azi}}[k] \otimes {}^{\mathcal{S}}_{\mathcal{E}}\boldsymbol{q}[k], \tag{1} $$

where ${}^{\mathcal{S}}_{\mathcal{A}}\boldsymbol{q}_{\mathrm{AF}}[k] \in \mathbb{H}$, $\left|{}^{\mathcal{S}}_{\mathcal{A}}\boldsymbol{q}_{\mathrm{AF}}[k]\right| = 1$ and $\mathbb{H}$ denotes the quaternion space. More precisely, ${}^{\mathcal{S}}_{\mathcal{A}}\boldsymbol{q}_{\mathrm{AF}}$ describes the inclination (azimuth-free part) of the sensor, because the azimuth of the frame $\mathcal{A}$ and the sensor frame $\mathcal{S}$ are well aligned. The quaternion

$$ {}^{\mathcal{A}}_{\mathcal{E}}\boldsymbol{q}_{\mathrm{azi}}[k] = \left[\cos\frac{\psi[k]}{2}, \underbrace{[0\,0\,1]}_{\mathcal{E}_z{}^T}\sin\frac{\psi[k]}{2}\right]^T \tag{2} $$

with ${}^{\mathcal{A}}_{\mathcal{E}}\boldsymbol{q}_{\mathrm{azi}}[k] \in \mathbb{H}$, $\left|{}^{\mathcal{A}}_{\mathcal{E}}\boldsymbol{q}_{\mathrm{azi}}[k]\right| = 1$ is defined as the azimuth part of the orientation using the azimuth rotation angle

$$ \begin{aligned} \psi[k] = \operatorname{atan2}(\, & 2q_1[k]q_2[k] + 2q_0[k]q_3[k], \\ & q_0^2[k] + q_1^2[k] - q_2^2[k] - q_3^2[k]), \\ \psi[k] \in\,]-\pi, \pi], & \end{aligned} \tag{3} $$

of the 1-2-3 Euler angle convention. Since only the inclination of the sensor is needed to calculate angles in the sagittal plane, the removal of azimuth increases robustness against azimuth drifts in the orientation and eliminates the necessity to use presumably disturbed magnetometer.

After a quaternion is available for each sensor, which describes the inclination, it is assumed that at least one full cycle movement has been done and hence, there is a set $\mathbb{S}_C$ of azimuth-free orientations ${}^{\mathcal{S}}_{\mathcal{A}}\boldsymbol{q}_{\mathrm{AF}}$ which represents one complete up and down motion of each sensor. Afterwards, the two quaternions with the maximum inclination angle difference of the set $\mathbb{S}_C$, ${}^{\mathcal{S}}_{\mathcal{A}}\boldsymbol{q}_{\mathrm{AF}}[u_{\max,0}]$ and ${}^{\mathcal{S}}_{\mathcal{A}}\boldsymbol{q}_{\mathrm{AF}}[u_{\max,1}]$, are searched. The rotation for the highest inclination difference can be calculated using these two quaternions by performing a quaternion multiplication:

$$\boldsymbol{q}_{\mathrm{MI}} = {}^{\mathcal{S}}_{\mathcal{A}}\boldsymbol{q}^{-1}_{\mathrm{AF}}[u_{\max,0}] \otimes {}^{\mathcal{S}}_{\mathcal{A}}\boldsymbol{q}_{\mathrm{AF}}[u_{\max,1}]. \tag{4}$$

The rotation axis can now be calculated with

$$\boldsymbol{x}_{\mathrm{d}} = \frac{V(\boldsymbol{q}_{\mathrm{MI}})}{\sin\left(\arccos(S(\boldsymbol{q}_{\mathrm{MI}}))\right)}, \quad \boldsymbol{x}_{\mathrm{d}} \in \mathbb{R}^3, \tag{5}$$

where $V()$ and $S()$ describe the vector and scalar part of a quaternion, respectively. Now, the angle around this axis can be calculated using

$$\gamma_{\boldsymbol{x}_{\mathrm{d}}} = 2\arctan\left(-\frac{\boldsymbol{x}_{\mathrm{d}} \cdot V\left({}^{\mathcal{S}}_{\mathcal{A}}\boldsymbol{q}_{\mathrm{AF}}[u]\right)}{S\left({}^{\mathcal{S}}_{\mathcal{A}}\boldsymbol{q}_{\mathrm{AF}}[u]\right)}\right). \tag{6}$$

By performing these operations for each set of IMU data and by applying the proposed geometric setting from Figure 1, the hip and knee joint angles $\hat{\varphi}_{H_L}$ and $\hat{\varphi}_{K_L}$ e.g. for left leg can be obtained with

$$\hat{\varphi}_{H_L} = \pi - \varphi_{IMU,T_L} - \gamma_{\mathrm{HAT}}, \tag{7}$$

$$\hat{\varphi}_{K_L} = \pi - \varphi_{IMU,T_L} - \varphi_{IMU,S_L}, \tag{8}$$

where the angle γ_{HAT} describes the pitch of the torso. In Figure 2, simulation results for the presented joint estimation method are displayed where the sensor's x-axis is placed 45° rotated with respect to the assumed hinge joint axis onto the segment (thigh) and an oscillation is applied to the hip joint. Further, after 15 s a sensor wobbling around the sensor's x-axis is added but the tracking error remains close to zero. Table I. summarizes the proposed method.

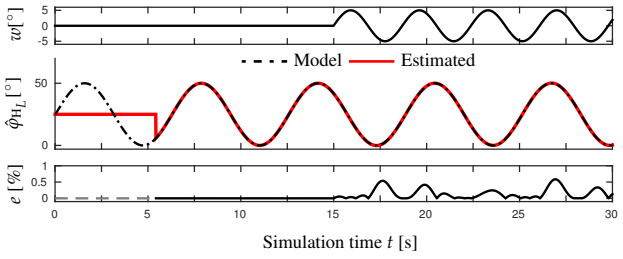

Figure 2: Joint angle estimation method. Top graph shows the applied sensor wobbling w. Middle graph shows the estimated joint angle $\hat{\varphi}_{\mathrm{H}}$ and the angle of the simulation model. Bottom graph shows the relative error e between the estimated angle and maximum amplitude of the reference angle. A sensor wobbling is applied after 15 s.

B. Joint angle based stimulation pattern generation

According to the model in [10], the contribution of each lower limp muscle used for FES cycling is categorized in Table II. Similar to the approaches in [2, 3, 4, 5], the quadriceps and hamstring are stimulated for their dominant function.

TABLE I. SUMMARY OF THE JOINT ANGLE ESTIMATION ALGORITHM. THE TABLE SHOWS THE REQUIRED INPUTS, THE CALCULATED OUTPUTS AS WELL AS THE SEQUENCE OF INSTRUCTIONS.

Inputs	acceleration $\boldsymbol{a}_i$ and angular rate $\boldsymbol{g}_i$ with $i = \{1..4\}$ of four inertial sensors

Algorithm	for every sample do:
	for every sensor do:
	estimate orientation ${}^{\mathcal{S}}_{\mathcal{E}}\boldsymbol{q}$
	calculate azimuth angle ψ
	calculate azimuth-free orientation ${}^{\mathcal{S}}_{\mathcal{A}}\boldsymbol{q}_A F$
	end for
	if a set $\mathbb{S}_C$ is complete:
	for every sensor do:
	search max inclination difference 1: ${}^{\mathcal{S}}_{\mathcal{A}}\boldsymbol{q}_{\mathrm{AF}}[u_{\max,0}]$
	search max inclination difference 2: ${}^{\mathcal{S}}_{\mathcal{A}}\boldsymbol{q}_{\mathrm{AF}}[u_{\max,1}]$
	calculate dominant rotation axis $\boldsymbol{x}_{\mathrm{d}}$
	calculate angle γ_i around axis $\boldsymbol{x}_{\mathrm{d}}$ using ${}^{\mathcal{S}}_{\mathcal{A}}\boldsymbol{q}_{\mathrm{AF}}$
	end for
	end if
	if γ_i is available for $i = \{1..4\}$:
	calculate joint angles $\hat{\varphi}_{\mathrm{H}}$ and $\hat{\varphi}_{\mathrm{K}}$ for both legs
	end if
	end for

Outputs	estimated joint angles: $\hat{\varphi}_{\mathrm{H}_R}$, $\hat{\varphi}_{\mathrm{H}_L}$, $\hat{\varphi}_{\mathrm{K}_R}$, $\hat{\varphi}_{\mathrm{K}_L}$

In contrast to crank-angle based stimulation pattern, the estimated joint angles shall be used to generate the stimulation pattern for each muscle and each leg. Therefore, the absolute joint angles are transformed to the fixed range of $[0;1[$ and denoted by the term cycling percentage (CP). The CP contains two sectors. For $0.0 \leq \mathrm{CP} < 0.5$, the joint is performing an extension motion and for $0.5 \leq \mathrm{CP} < 1.0$, the joint is performing a flexion motion. The mapping offers the possibility to determine joint flexion and extension independent of the seating position or geometry (e.g. thigh lengths, distance of the seat to crank).

TABLE II. FUNCTION AND DOMINANCE OF THE USED MUSCLE GROUPS. THE FUNCTION CAN BE EXTRACTED FROM THE MODEL USED IN [10]. THE LAST COLUMN SHOWS THE PROPOSED STIMULATION INTERVALS IN THE CP SIGNAL WITH $s \in \{L, R\}$.

Muscle group	Muscles	Function	Dominance	Stimulation
Quadriceps	Rectus fermoris	Knee extension	Knee extension	$\hat{\varphi}^{\mathrm{CP}}_{\mathrm{K}_s} \in [0.0, 0.4]$
	Vasti	Hip flexion		
Hamstring	Hamstring	Knee flexion	Knee flexion	$\hat{\varphi}^{\mathrm{CP}}_{\mathrm{K}_s} \in [0.5, 1.0]$
	Biceps fermoris	Hip extension		$\hat{\varphi}^{\mathrm{CP}}_{\mathrm{H}_s} \in [0.0, 0.6]$

In order to generate the CP signal, the joint angle estimations are searched for their maximum and minimum continuously since the joint angle trajectory during cycling can be approximated by an oscillation but the amplitude and offset of the oscillation is changing due to disturbances, e.g. sliding on the seat and sensor wobbling. The maximum and minimum is used to bound the joint angle signal before transforming it into a signal similar to a saw tooth signal. The transformation is defined as follows:

$$\varphi^{\mathrm{CP}}[k] = \begin{cases} \frac{1}{2}\frac{\varphi - p_{\mathrm{b}}}{p_{\mathrm{t}} - p_{\mathrm{b}}}, & \text{for} \quad \frac{\dot{\varphi}[k]}{p_{\mathrm{t}} - p_{\mathrm{b}}} > 0 \\ 1 - \frac{1}{2}\frac{\varphi - p_{\mathrm{b}}}{p_{\mathrm{t}} - p_{\mathrm{b}}} & \text{for} \quad \frac{\dot{\varphi}[k]}{p_{\mathrm{t}} - p_{\mathrm{b}}} \leq 0 \end{cases}, \tag{9}$$

where $p_{\mathrm{t}} \in \mathbb{R}$ is the current maximum peak and $p_{\mathrm{b}} \in \mathbb{R}$ the current minimum peak. To avoid high switching frequencies at the turning points a small hysteresis is included into the transformation. An exemplary transformation is shown in Figure 3.

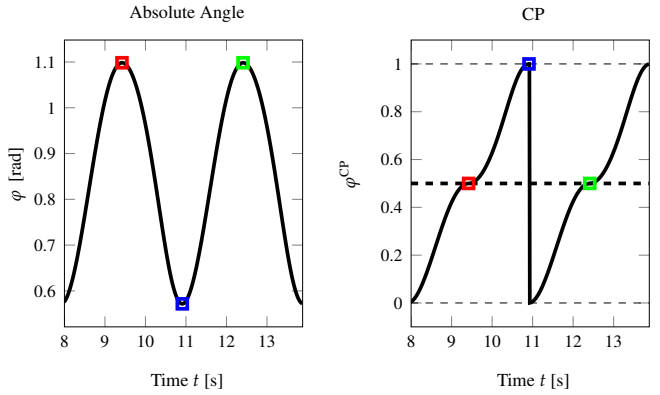

Figure 3: Joint angle signal processing. Left: Absolute joint angle (black, solid) with detected peaks (red, blue and green squares). Right: Cycling Percentage (black, solid) with corresponding peaks (red, blue and green squares) and a sector border.

C. *Speed compensation methods*

The proposed static stimulation pattern activates the stimulation according to a functional objective. The dynamic muscle force response of the muscles results in a delay between stimulation onset and force reaction. This makes it necessary to apply a correction so as to ensure that the muscle generates force in the desired joint angle ranges. A mean speed-based correction which is described in [1] for a crank angle-based approach is adapted for the use of joint angles. Therein, the mean cycling speed is used to shift the static stimulation pattern against the cycling direction. A latency time of 130 ms is proposed in [1] for the muscle force response. This kind of corrections shifts slow parts of the signal more than fast parts with respect to the time which unintentionally lead to different stimulation interval length compared to the static pattern. The improvement of this method will be subject of future works.

III. Simulation Model and Results

A biomechanical model, which is shown in Figure 4, is used to obtain simulation results for the presented methods. The modelling of the muscles and their answer to FES is based on [10]. Within the model the same muscles compared to the experiment can be activated based on FES using a combination of pulse width $\varrho(t)$ and stimulation frequency $f_{\text{stim}}(t)$. Active and passive moments for the lower limb joints are then calculated and applied to a mechanical model which is created using the simulation framework SimMechanics™. The model covers a mechanical representation of a cycling motion for the lower limbs providing joint motion, crank angle, cadence and sensor data of virtual inertial sensors placed on the virtual thighs and shanks. The output of the inertial sensors is used to test the presented methods, i.e. estimating joint angles and generating a stimulation timing.

A simulation (Figure 5) is carried out to validate that the presented methods are capable of inducing a cycling motion without manual tuning despite changing geometric parametrizations. Therefore, the seat position of the model is varied in distance and height (with respect to the crank). Additionally, a simple PI controller is used to control the mean cycling speed to 60 rpm by controlling the pulse width and keeping $f_{\text{stim}}(t)$ constant. First of all, the joint angle-based approach is able to induce a cycling motion using the proposed pattern despite

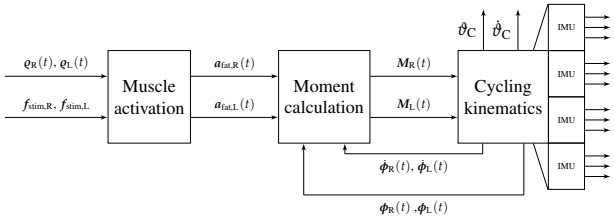

Figure 4: Structure of the simulation model. Pulse width and stimulation frequency are used as inputs to generate the crank angle ϑ_C and cadence $\dot{\vartheta}_C$. Attached virtual inertial sensors generate sensor data based on a mechanics simulation.

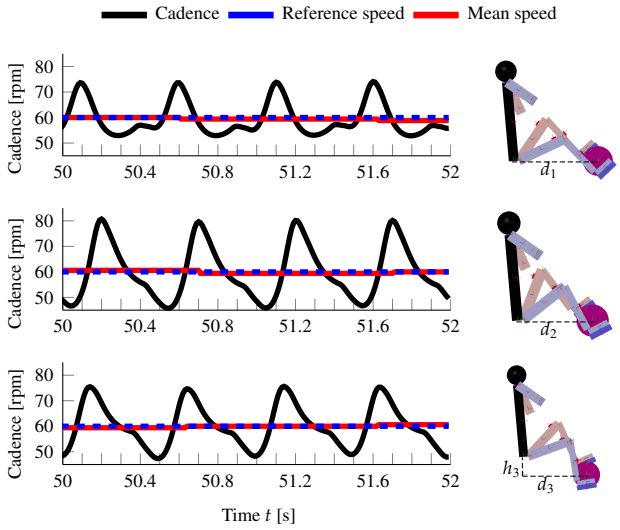

Figure 5: Cycling simulation for the joint angle-based approach using different geometric parameterization using the correction method. The crank cadence, the mean cycling speed, and the reference speed are visualized for every simulation. Geometric parameters: $d_1 = 0.85\,\text{m}$, $d_2 = 0.70\,\text{m}$, $d_3 = 0.70\,\text{m}$, $h_3 = 0.20\,\text{m}$.

the geometry changes. Further, it is possible to influence the mean speed and control it to the desired value by changing the stimulation intensity. This confirms that the joint angle estimation and cycling percentage mapping are independent of the geometry without the need for manual pattern tuning.
Furthermore, the simulation result shows that the cadence smoothness (smooth is meant to be a low deviation from the mean cadence value) depends on the seat position and thus, on the distance. While inducing a cycling motion is still possible, sitting too close to the crank decreases the cycling quality by means of cadence smoothness, due to the changed lever arm relation. Controlling and improving the cadence smoothness is not part of this work and will be discussed in future works.

IV. Experimental Setup and Results

All experiments were done with one paraplegic subject who is training for the Cybathlon 2016 under medical supervision of the Unfallkrankenhaus Berlin. The participant gave written informed consent received. The experimental set-up is shown in Figure 6. Four IMUs (MTw, Xsens Technologies B.V., Netherlands) are placed on the lower limbs, one per shank and one per thigh. The acceleration and gyroscope data is transferred wirelessly to a receiver connected to a control unit (laptop, Ubuntu 14.04). The laptop performs the joint angle estimation and generates the stimulation timing based on a

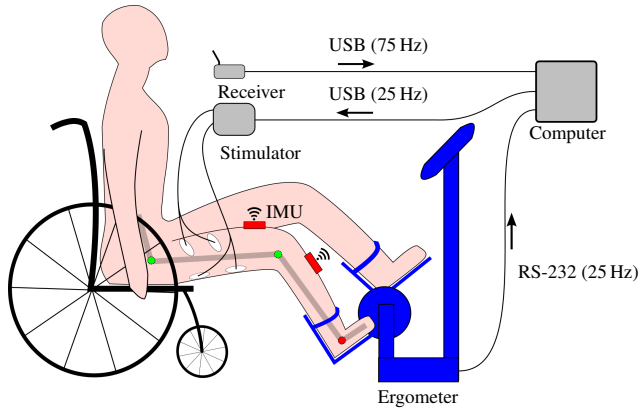

Figure 6: Overview of the experimental structure. IMUs are placed on the thigh and shank. Paraplegic individual is sitting in a wheelchair in front of an ergometer (Motomed viva2).

pattern. The desired pulse width and current are transferred to the stimulator (RehaStim, Hasomed GmbH) and applied to adhesive transcutaneous electrodes placed on the hamstring and quadriceps muscle groups. The ankle joints are stabilized by the ergometer's foot shells. The cadence recorded by the ergometer is saved for comparability purposes only and thus, it is not used to for FES cycling.

For the experiment, the ergometer is configured to ensure a cycling speed of 12 rpm by utilizing its motor. When the patient is cycling by himself the ergometer automatically switches to a mode where it applies a constant load (isotonic training). After some initial cycles, it was ensured that the joint angle estimation is working correctly before raising the stimulation current. Figure 7 shows the cadence and stimulation current. Raising the stimulation current induces an acceleration of the cycling motion. This implies that FES cycling using simple joint angle-driven stimulation pattern without manual tuning is possible.

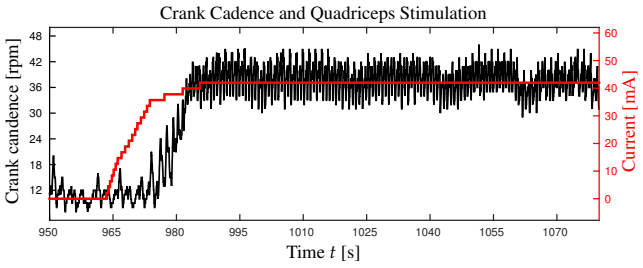

Figure 7: Experiment using a joint angle-based stimulation pattern with a paraplegic subject (ASIA impairment Scale A, Sub Th5, prior 4 weeks training with RehaMove and ergometer). Stimulation was running at a frequency of 25 Hz with standard biphasic pulses. Crank cadence (black) and the applied stimulation current (red) are shown. Pulse width and frequency of stimulation are constant. A rise of the stimulation current induces a cycling motion with fixed pulse width of 350 μs

V. Conclusion

A new concept for FES cycling was proposed which uses a joint angle estimation to control the stimulation instead of the crank angle as in the current state-of-the-art technology. The novel approach offers a plug & play system without the need for an initial calibration or manual tuning. Therefore, a method was introduced which offers joint angle estimates of the hip and knee joints by utilizing IMUs on the shank and thigh. The presented methods enable arbitrary sensor-to-segment placement by performing a rotation axis identification. Then, a simple joint angle transformation is introduced to drive stimulation patterns independent of the geometric parameterization. By using a simple stimulation pattern, simulations proofed the concept. Finally, it was shown that the novel approach works in a real experiment with a paraplegic individual. The proposed FES cycling system was able to induce an acceleration and to maintain cycling. It offers advantages like device flexibility and set-up time reduction by offering a plug & play usage.

Future research should aim at reducing the effects of sensor wobbling, e.g. by improving the IMU attachment. Further, the muscle force response compensation should be improved to make the cycling experience smoother with respect to the cadence trajectory. A method to calculate the crank angle by using the joint angle estimates should be considered to ensure compatibility and comparability to state-of-the-art technologies in FES cycling.

Acknowledgment

We would like to acknowledge Axelgaard Manufacturing Co., USA for donating the used stimulation electrodes.

References

[1] T. Schauer, *Feedback Control of Cycling in spinal cord injury using functional electrical stimulation.* PhD thesis, 2005.

[2] A. Farhoud and A. Erfanian, "Higher-order sliding mode control of leg power in paraplegic FES-cycling," *2010 Annual International Conference of the IEEE Engineering in Medicine and Biology Society, EMBC'10*, pp. 5891–5894, 2010.

[3] T. Watanabe, T. Murakami, and Y. Handa, "Preliminary Tests of a Prototype FES Control System for Cycling Wheelchair Rehabilitation," *IEEE International Conference on Rehabilitation Robotics*, 2013.

[4] S. C. Abdulla and M. O. Tokhi, "Optimization of indoor FES-cycling exercise assisted by a flywheel mechanism using genetic algorithm," *2014 IEEE International Symposium on Intelligent Control (ISIC)*, pp. 1867–1871, 2014.

[5] M. Bellman, T.-H. Cheng, R. Downey, and W. Dixon, "Cadence control of stationary cycling induced by switched functional electrical stimulation control," in *Decision and Control (CDC), 2014 IEEE 53rd Annual Conference on*, pp. 6260–6265, Dec 2014.

[6] P. D. Faghri, R. M. Glaser, and S. F. Figoni, "Functional electrical stimulation leg cycle ergometer exercise: Training effects on cardiorespiratory responses of spinal cord injured at rest and during submaximal exercise," *Arch. Phys. Med. Rehab.*, vol. 73, pp. 1085–1093, 1992.

[7] S. Ferrante, B. Saunders, L. Duffell, A. Pedrocchi, K. Hunt, T. Perkins, and N. Donaldson, "Quantitative evaluation of stimulation patterns for fes cycling," *10th Annual Conference of the International FES Society*, 2005.

[8] K. J. Hunt, C. Ferrario, S. Grant, B. Stone, A. McLean, M. Fraser, and D. B. Allan, "Comparison of stimulation patterns for fes-cycling using measures of oxygen cost and stimulation cost," *Med Eng Phys*, vol. 28, pp. 710–8, 2006.

[9] T. Seel, F. Peter, L. Landgraf, and T. Schauer, "Using IMUs for Measuring Body Segment Orientations in Indoor Environments," Technically Assisted Rehabilitation (TAR), Berlin, 2015.

[10] R. Riener and T. Fuhr, "Patient-Driven Control of FES-Supported Standing Up: A Simulation Study," *IEEE Tranactions on Rehabilitation Engineering*, vol. 6, no. 2, 1998.